AMERICAN SOCIETY FOR MICROBIOLOGY | Antimicrobial Agents and Chemotherapy®

MECHANISMS OF RESISTANCE

Characterization of the AmpC β-Lactamase from *Burkholderia multivorans*

Scott A. Becka,[a] Elise T. Zeiser,[a] Melissa D. Barnes,[a,b] Magdalena A. Taracila,[a,b] Kevin Nguyen,[e] Indresh Singh,[e] Granger G. Sutton,[e] John J. LiPuma,[d] Derrick E. Fouts,[e] Krisztina M. Papp-Wallace[a,b,c]

[a]Research Service, Louis Stokes Cleveland Department of Veterans Affairs, Cleveland, Ohio, USA

[b]Department of Medicine, Case Western Reserve University, Cleveland, Ohio, USA

[c]Department of Biochemistry, Case Western Reserve University, Cleveland, Ohio, USA

[d]Department of Pediatrics and Communicable Disease, University of Michigan Medical School, Ann Arbor, Michigan, USA

[e]J. Craig Venter Institute, Rockville, Maryland, USA

ABSTRACT *Burkholderia multivorans* is a member of the *Burkholderia cepacia* complex, a group of >20 related species of nosocomial pathogens that commonly infect individuals suffering from cystic fibrosis. β-Lactam antibiotics are recommended as therapy for infections due to *B. multivorans*, which possesses two β-lactamase genes, bla_{penA} and bla_{AmpC}. PenA is a carbapenemase with a substrate profile similar to that of the *Klebsiella pneumoniae* carbapenemase (KPC); in addition, expression of PenA is inducible by β-lactams in *B. multivorans*. Here, we characterize AmpC from *B. multivorans* ATCC 17616. AmpC possesses only 38 to 46% protein identity with non-*Burkholderia* AmpC proteins (e.g., PDC-1 and CMY-2). Among 49 clinical isolates of *B. multivorans*, we identified 27 different AmpC variants. Some variants possessed single amino acid substitutions within critical active-site motifs (Ω loop and R2 loop). Purified AmpC1 demonstrated minimal measurable catalytic activity toward β-lactams (i.e., nitrocefin and cephalothin). Moreover, avibactam was a poor inhibitor of AmpC1 ($K_{i\ app}$ > 600 μM), and acyl-enzyme complex formation with AmpC1 was slow, likely due to lack of productive interactions with active-site residues. Interestingly, immunoblotting using a polyclonal anti-AmpC antibody revealed that protein expression of AmpC1 was inducible in *B. multivorans* ATCC 17616 after growth in subinhibitory concentrations of imipenem (1 μg/ml). AmpC is a unique inducible class C cephalosporinase that may play an ancillary role in *B. multivorans* compared to PenA, which is the dominant β-lactamase in *B. multivorans* ATCC 17616.

KEYWORDS β-lactamases, *Burkholderia*, β-lactam, AmpC

Burkholderia multivorans is a member of a larger group of pathogens, the *Burkholderia cepacia* complex (BCC), that includes >20 different species (1, 2). BCC bacteria can cause infections (e.g., pneumonia) in immunocompromised persons or in other individuals, such as those with cystic fibrosis (3–7). Currently, β-lactam antibiotics are recommended as a treatment option for infections due to BCC bacteria (8, 9). However, BCC bacteria are inherently resistant to multiple antibiotics, including β-lactams, in which the mechanistic basis for resistance is correlated with the expression of β-lactamases (10–13).

β-Lactamases are clustered into four-different classes based on structural similarities (classes A, B, C, and D) (14). Class A, C, and D β-lactamases use a serine as the nucleophile, while class B β-lactamases are metalloenzymes, using a Zn^{2+} ion(s) for catalysis. Analysis of the *B. multivorans* ATCC 17616 genome revealed the presence of two β-lactamases: PenA, a class A β-lactamase, and AmpC, a class C β-lactamase (Table 1) (15). A LysR-type transcriptional regulator ($PenR_A$) is upstream of bla_{PenA} and is

Received 1 June 2018 **Returned for modification** 18 June 2018 **Accepted** 7 July 2018

Accepted manuscript posted online 16 July 2018

Citation Becka SA, Zeiser ET, Barnes MD, Taracila MA, Nguyen K, Singh I, Sutton GG, LiPuma JJ, Fouts DE, Papp-Wallace KM. 2018. Characterization of the AmpC β-lactamase from *Burkholderia multivorans*. Antimicrob Agents Chemother 62:e01140-18. https://doi.org/10.1128/AAC.01140-18.

Address correspondence to Krisztina M. Papp-Wallace, krisztina.papp@va.gov.

TABLE 1 Annotated β-lactamases in the *B. multivorans* ATCC 17616 genome

No.	Locus tag; locus; chromosome	Class	Assessment
1	BMUL_RS18715; NC_010086; 2	A	PenA; possesses a signal peptide, SXXK, SDN, and KTG motifs
2	BMUL_RS20495; NC_010086; 2	A	Possesses a signal peptide but lacks SXXK, SDN, and KTG motifs
3	BMUL_RS30175; NC_010087; 3	C	AmpC1; possesses a signal peptide, SXXK, YSN, and KTG motifs

divergently transcribed. Expression of bla_{PenA} is regulated by $PenR_A$ through a system analogous to AmpC/AmpR regulatory pathways present in *Enterobacteriaceae* and *Pseudomonas aeruginosa* (13, 16).

PenA was previously characterized and found to possess a very broad hydrolytic profile that includes penicillins, cephalosporins, carbapenems, and the monobactam aztreonam, as well as the β-lactamase inhibitors clavulanic acid, sulbactam, and tazobactam (17). In addition, PenA demonstrated significant sequence heterogeneity within clinical isolates of *B. multivorans* (18). Here, we analyze the second β-lactamase present in *B. multivorans* ATCC 17616, AmpC1. Similarly to PenA, AmpC also displays sequence diversity within clinical isolates of *B. multivorans*. Conversely, AmpC1 from *B. multivorans* ATCC 17616 possesses a narrow spectrum, and the contribution of AmpC1 to β-lactam resistance appears to be negligible, yet expression of AmpC1 is regulated by β-lactam inducers (e.g., imipenem).

RESULTS AND DISCUSSION

The amino acid sequence of AmpC is diverse compared to those of other AmpC β-lactamases, but the structure is similar. AmpC possesses the classic motifs (SXXK, YSN, Ω loop, KTG, and R2 loop) found in other AmpC proteins (Fig. 1A). However, AmpC is most similar to other *Burkholderia* AmpC proteins (75% identity and 80% homology to *Burkholderia cenocepacia* AmpC [BcAmpC]) (Fig. 1B). Comparisons to prevalent chromosomal (*Pseudomonas*-derived cephalosporinase 1 [PDC-1], *Acinetobacter*-derived cephalosporinase 1 [ADC-1], P99 [*Enterobacter cloacae* AmpC], and *Escherichia coli* AmpC) and plasmidic (CMY-2 and FOX-4) AmpC proteins reveal lower identity (38 to 46%) and homology (58 to 61%) (Fig. 1B).

Two homology models of AmpC1 were generated using the *B. cenocepacia* AmpC crystal structure (Protein Data Bank [PDB] accession no. 5E2G). AmpC1 maintains the expected class C β-lactamase structure; however, the positioning of Q120 in the loop (residues L117 to H126) was nearly 5 Å away from the nucleophilic S64 unlike other AmpC proteins (i.e., CMY-2) (Fig. 2A, purple). The 500-ps molecular dynamics simulation (MDS) of the generated models revealed that the loop region is highly mobile, shifting 10 Å (Fig. 2A, yellow). The second homology model of AmpC1 shows that the loop between residues L117 and H126 was found in a different position (Fig. 2A, magenta). Further refinement of this loop region in AmpC1 was conducted in order to find the most favorable conformation. The loop's energy was optimized using the *ab initio* loop prediction algorithm LOOPER. The most energetically favorable conformation of the loop was most similar to model 2 (Fig. 2A, cyan). Efforts are under way to determine the crystal structure of AmpC1 to provide additional information on the positioning of the loop.

AmpC of *B. multivorans* exhibits considerable sequence heterogeneity. To determine the sequence diversity of AmpC in *B. multivorans*, we analyzed the primary amino acid sequence of AmpC proteins from 49 different clinical isolates, and 27 novel AmpC variants were identified (Table 2). The variants had 1 to as many as 13 different amino acid substitutions. The locations of these amino acid substitutions were mapped to the AmpC1 homology model (Fig. 2B). The amino acid substitutions included those in the Ω loop (D193A, R196S, and T205A), as well as the R2 loop (K290T) (Fig. 2B). Amino acid substitutions in the Ω loop and the R2 loop of other AmpC proteins were shown

A.

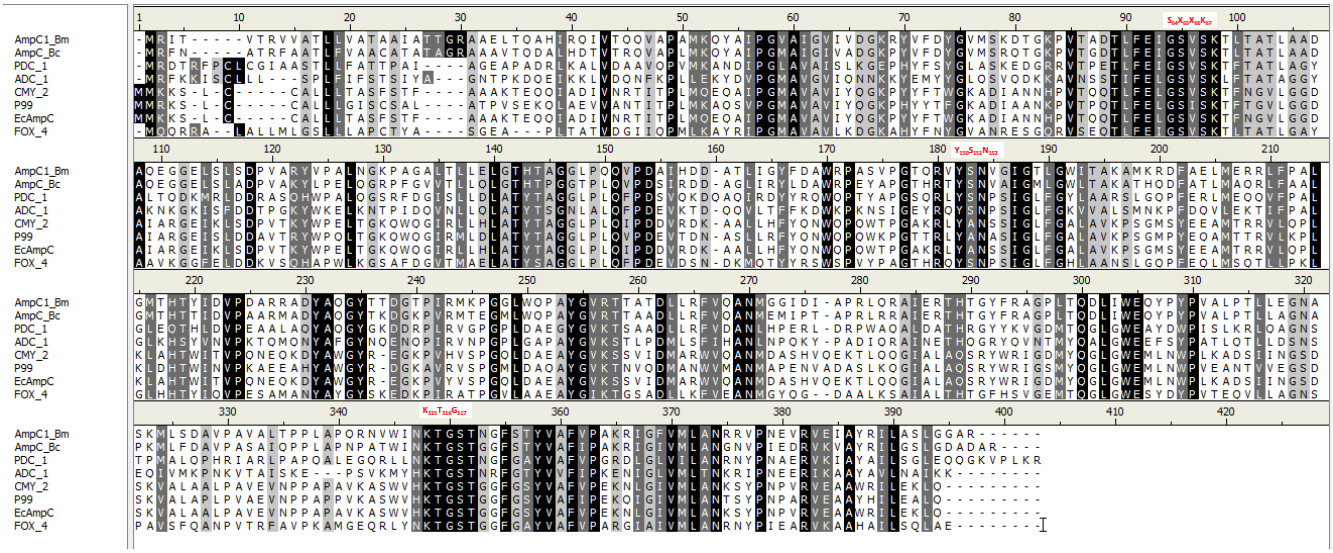

B.

Protein	% Identity	% Homology
B. cenocepacia AmpC	75	80
PDC-1	44	61
CMY-2	42	59
E. coli AmpC (EcAmpC)	42	59
FOX-4	46	61
ADC-1	38	58
P99	42	59

FIG 1 Comparison of AmpC1 from *B. multivorans* (AmpC1_Bm) with AmpC from *B. cenocepacia* J2315 (AmpC_Bc) and other prevalent class C β-lactamases (PDC_1 and *E. coli* AmpC [EcAmpC]). (A) Amino acid sequence alignments using Clustal Ω. Black shading indicates identity, dark-gray shading is similarity, and light-gray and white shading are differences. AmpC motifs (SXXK, YSN, and KTG) are in red. (B) Percent identity and homology between prevalent AmpC proteins and AmpC1.

to confer extended-spectrum AmpC phenotypes (e.g., the ability to hydrolyze cefotaxime and ceftazidime) (19).

AmpC1 possesses a narrow spectrum for β-lactams. To assess the contribution of AmpC1 to β-lactam resistance, the bla_{AmpC1} gene was cloned into pBC SK(+) and expressed in *E. coli* DH10B for susceptibility testing and was cloned into the pGEX-6p-2 plasmid and expressed in *E. coli* Rosetta-gami 2 DE3 for protein purification and kinetics. In addition, the bla_{AmpC1} gene was knocked out of *B. multivorans* ATCC 17616 using allelic replacement followed by subsequent excision via recombination. The bla_{AmpC1} knockout strain was verified by PCR, and the phenotypic verification is presented in Fig. S1 in the supplemental material. An analytic isoelectric focusing (aIEF) gel overlaid with nitrocefin revealed the absence of AmpC1 activity in the knockout compared to the parental strain.

Susceptibility testing was conducted via disk diffusion and Etest using a panel of select β-lactams (e.g., ampicillin, cephalothin, ceftriaxone, cefotaxime, ceftazidime, and imipenem) (see Fig. S2A in the supplemental material). *E. coli* producing bla_{AmpC1} was highly susceptible to all the agents tested, with only minor nonsusceptibility observed for cephalothin, with an intermediate zone of 17 mm (see Fig. S2B in the supplemental material). Subsequently, *E. coli* bacteria producing bla_{AmpC1}, along with *B. multivorans* ATCC 17616 Δbla_{AmpC1}, were subjected to MIC determination via agar dilution. Control strains, including *B. multivorans* ATCC 17616 and *E. coli* DH10B pBC SK(+) with bla_{PenA}, as well as an empty vector, were also tested. *B. multivorans* ATCC 17616 was highly

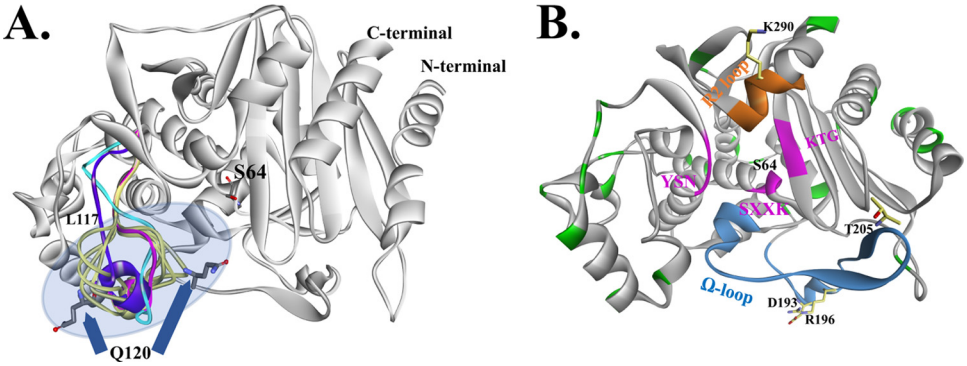

FIG 2 (A) Homology models of AmpC1 combined with a loop refinement protocol suggest high flexibility of the L117-to-H126 loop (model 1, purple; model 2, cyan; multiple possible conformations from loop refinement, yellow; best energetically favorable conformation, magenta). The Q120 region has the largest movement (up to 10 Å), possibly changing the shape of the active-site entrance. (B) The amino acids that are replaced in the 27 AmpC variants (Table 2) are highlighted in green. Natural variants of AmpC have amino acid substitutions in two active-site motifs, the Ω loop (blue) (residues D193, R196, and T205) and the R2 loop (orange) (position K290); other active-site regions are the SXXK (with the nucleophilic S64), YSN, and KTG motifs (pink).

resistant to all of the β-lactams (i.e., ampicillin, cephalothin, and imipenem) tested, and susceptibility to ampicillin was restored with avibactam, as expected from our previous work (Table 3) (20).

The MICs of ampicillin, cephalothin, and imipenem for *B. multivorans* ATCC 17616 Δbla_{AmpC1} were equivalent to those for the parent strain (Table 3). Moreover, *E. coli* with bla_{AmpC1} was susceptible to ampicillin (MIC = 8 μg/ml) and imipenem (MIC = 1 μg/ml) but demonstrated resistance to cephalothin (MIC = 32 μg/ml) (Table 3). The observations with AmpC1 are in sharp contrast to those for *E. coli* producing bla_{PenA}. The MICs for *E. coli* carrying bla_{PenA} more closely mimicked those of the parent strain, *B. multivorans* ATCC 17616, with nonsusceptibility to all the agents tested and susceptibility restored with the addition of avibactam (Table 3). The susceptibility testing results suggest that bla_{PenA} contributes significantly to β-lactam resistance in *B. multivorans*, while AmpC1 plays a minor role.

AmpC proteins typically demonstrate catalytic efficiencies near the diffusion limit (10^9 M^{-1} s^{-1}) for select cephalosporins (e.g., cephalothin) (21). Avibactam, a novel β-lactamase inhibitor of the diazabicyclooctane family, inactivates class A, class C, and some class D β-lactamases and, in combination with ceftazidime, restores susceptibility to ceftazidime against *B. multivorans* (20). Steady-state kinetics were conducted with a panel of β-lactams to evaluate the hydrolytic profile of purified AmpC1, as well as with the β-lactamase inhibitor, avibactam, to assess the ability of avibactam to inactivate AmpC1.

The purified AmpC1 β-lactamase was able to appreciably hydrolyze only cephalothin and nitrocefin; all other β-lactam substrates were not measurably hydrolyzed (see Fig. S2C in the supplemental material). AmpC1 showed high K_m values for nitrocefin (176 ± 36 μM) and cephalothin (392 ± 88 μM) (Table 4). However, the k_{cat} value for nitrocefin was considerable, resulting in a catalytic efficiency of 1.4 ± 0.3 μM^{-1} s^{-1}, which is only ~2-fold lower than that for PenA (Table 4). The catalytic efficiency for cephalothin was ~30-fold lower for AmpC1 than for PenA (Table 4). AmpC1 is able to hydrolyze select cephalosporins, but not nearly as well as other AmpC proteins (19). In *B. multivorans*, PenA is a more efficient β-lactamase than AmpC.

Avibactam is a potent inhibitor of PenA (apparent K_i [$K_{i\ app}$] = 500 nM) (Table 4) (20). Conversely, the $K_{i\ app}$ endpoint (>600 μM) for AmpC1 could not be determined due to the poor inhibitory activity of avibactam against AmpC1 (Table 4).

Avibactam is able to form an acyl complex with AmpC1. To determine whether avibactam is able to acylate AmpC1, electrospray ionization-mass spectrometry (ESI-MS) was conducted on AmpC1 incubated at 1:1 and 1:10 AmpC1/avibactam ratios with reactions terminated at 15 min and 24 h. The calculated molecular mass for AmpC1 is

TABLE 2 Single amino acid substitutions found in AmpC proteins from 46 clinical isolates of *B. multivorans*[a]

Strain(s)	Amino acid substitution(s), insertion(s), or deletion(s)	No. of differences	Refseq protein accession no.	AmpC designation
ATCC 17616, AU21747, AU17545, AU19729, AU10398, AU19518, AU14371, AU28069, AU25543, AU30760, AU20929		0	WP_012218336.1	AmpC1
AU19564	L104P	1	WP_105845787.1	AmpC2
AU13919, AU14328	T229V, G241A, R309P	3	WP_105776316.1	AmpC3
AU10897	G98A, T229V, K290T, A363E	4	WP_105758864.1	AmpC4
AU17534	D76A, T229A, G241A, K290T	4	WP_105783420.1	AmpC5
AU23995	A129V, R139H, T229A, I244T, A363E	5	WP_105810139.1	AmpC6
AU4507	A74V, R176Q, T229A, G241A, A363E	5	WP_006416937.1	AmpC7
AU24277	P18S, T205A, T229A, I244T, A363E	5	WP_105835089.1	AmpC8
AU12481	A137T, T205A, T229A, I244T, R261Q	5	WP_105789398.1	AmpC9
AU29198	TL11 M, T229A, D230E, K290T, P304S	5	WP_105844745.1	AmpC10
AU23668	L104V, A124E, V143 M, T229A, G362D, A363E	6	WP_105813500.1	AmpC11
AU14364	TL16S, T4A, T229A, G241A, G362D, A363E	6	WP_105765510.1	AmpC12
AU11233	TL11S, I11F, I33V, E79Q, M184L, T229A, I244T	7	WP_105770301.1	AmpC13
AU26250, AU15954, AU22892	TL11 M, V89I, R196S, T229V, I244T, K290T, A363E	7	WP_105780250.1	AmpC14
AU15814	TL16S, T4A, T111A, T229A, G241A, G362D, A363E	7	WP_105764661.1	AmpC15
AU30441	H7R, I8V, S47A, A141V, T229A, G241A, Q249R, A363D	8	WP_105811053.1	AmpC16
AU30050	S47A, A141V, D193A, T205A, T229A, G241A, Q249R, A363D	8	WP_105793891.1	AmpC17
AU21015	I8V, P18S, A165S, D190N, T205A, T229V, I245T, R309P	8	WP_107998461.1	AmpC18
AU14786, AU11772, AU23919	A17V, S47A, A141V, D193A, T205A, T229A, G241A, Q249R, A363D	9	WP_105767194.1	AmpC19
AU11358	TL22S, H7R, I8V, S47A, A141V, T205A, T229A, G241A, Q249R, A363D	10	WP_105775307.1	AmpC20
AU22436	H7R, I8V, S47A, A141V, D193A, T205A, T229A, G241A, Q249R, A363D	10	WP_006405341.1	AmpC21
AU17135, AU10047, AU28442	H7R, I8V, S47A, A141V, D193A, T229A, G241A, Q249R, P281S, I352 M, A363E	11	WP_105752596.1	AmpC22
AU16734	H7R, I8V, S47A, A141V, D193A, T229A, G241A, Q249R, P281S, L305R, A363E	11	WP_105792096.1	AmpC23
AU23690, AU11204	TL22S, H7R, I8V, S47A, A141V, D193A, T229A, G241A, Q249R, P281S, A363E	11	WP_105761708.1	AmpC24
AU19659	H7R, I8V, S47A, A141V, D193A, T205A, T229A, G241A, Q249R, P281S, L305R, A363E	12	WP_105807900.1	AmpC25
AU30438	TL22S, H7R, I8V, S47A, A141V, D193A, T205A, T229A, G241A, Q249R, V278I, A363E	12	WP_105847138.1	AmpC26
AU25057	TL22S, H7R, I8V, S47A, A141V, D193A, T205A, T229A, G241A, Q249R, P281S, A363E	12	WP_105838144.1	AmpC27
AU27706, AU23365	TL22S, H7R, I8V, I11V, S47A, A141V, D193A, T205A, T229A, G241A, Q249R, A279E, A363E	13	WP_069221591.1	AmpC28
AU18096, AU21596, AU10086	No class C β-lactamase found			

[a]The AmpC sequences were compared to that of AmpC1 from *B. multivorans* ATCC 17616.

39,748.61 Da, and the theoretical molecular mass for avibactam is 265 Da. The measured masses of apo-AmpC1 were 39,748 ± 5 Da and 39,747 ± 5 Da after 15-min and 24-h incubations (Fig. 3A and B). After a 15-min incubation with avibactam at a 1:1 ratio, only apoenzyme (39,748 Da) was observed; however, at a 1:10 ratio, small amounts of acyl-AmpC1 (40,014 ± 5 Da and 39,933 ± 5 Da) were observed (Fig. 3A and B). The 40,014- ± 5-Da peak corresponds to the addition of the unmodified avibactam (+265 Da) to AmpC1. The 39,933- ± 5-Da peak is also an acyl adduct; however, the mass is decreased by 80 Da, suggestive of the desulfated form of avibactam bound to AmpC1 (22). At 24 h, the acyl complex of AmpC1-avibactam (40,012 ± 5 Da) predominates at both 1:1 and 1:10 ratios (Fig. 3A and B). The desulfated avibactam-acyl complex (39,932 ± 5 Da) is observed in both; in addition, a new minor peak of 39,729 ± 5 Da was observed at the 24-h time point. The 39,729- ± 5-Da peak differs from that of apo-AmpC1 (39,748 Da) by −19 Da, suggestive of loss of a water molecule. Further analysis is under way to determine the significance of this peak. Avibactam is able to acylate AmpC1; however, the kinetic and ESI-MS data suggest that the rate is very low. Conversely, PenA forms an acyl-enzyme complex with avibactam within 15 s of incubation, as detected via ESI-MS (20).

TABLE 3 Susceptibility testing results

Strain	MIC (μg/ml)			
	Ampicillin	Ampicillin-avibactam[a]	Cephalothin	Imipenem
B. multivorans				
ATCC 17616	1,024	4	≥4,096	64
ATCC 17616 Δbla_{AmpC1}	1,024	4	≥4,096	64
E. coli				
DH10B pBC SK(+)	2	1	2	1
DH10B pBC SK(+) bla_{PenA}	4,096	4	4,096	2
DH10B pBC SK(+) bla_{AmpC1}	8	4	32	1

[a]Ampicillin was varied, and avibactam was held at a constant concentration of 4 μg/ml. CLSI interpretive indices were as follows: *Enterobacteriaceae* (ampicillin, ≥32 μg/ml, resistant; cephalothin, ≥32 μg/ml, resistant; imipenem, ≥4 μg/ml, resistant; and imipenem, 2 μg/ml, intermediate), nonfermenting Gram-negative bacteria (penicillins, ≥128 μg/ml, resistant; cephalosporins, ≥32 to 64 μg/ml, resistant; and carbapenems, ≥8 to 16 μg/ml, resistant).

Avibactam forms unfavorable complexes with AmpC1. Using the homology model of AmpC1 with the more energetically favorable conformation of the L117-to-H126 loop, avibactam was docked into the active site. The active-site pocket of AmpC1 is a deep, narrow groove, resulting in avibactam clashing with some of the side chains during entry into the active site. In the Michaelis-Menten complex of avibactam in AmpC1, the carbonyl of avibactam is positioned in the oxyanion hole (i.e., backbone amides of S64 and S318). However, the carbamate moiety of avibactam is within hydrogen-bonding distance of active-site residues S64, K67, and N152, which decreases the probability of acylation (Fig. 4). The active-site pocket is constraining, preventing productive interactions. The observations of molecular modeling support the high $K_{i\ app}$ of avibactam for AmpC1.

The morphology of *B. multivorans* Δbla_{AmpC1} is similar to that of wild-type cells. To assess if knocking out bla_{AmpC1} alters the overall cell shape, *B. multivorans* ATCC 17616 and the Δbla_{AmpC1} strains were stained using BacLight LIVE/DEAD staining and viewed using fluorescence microscopy. The morphology of the Δbla_{AmpC1} strain was very similar to that of the wild type; thus, lack of AmpC1 does not affect the cell's shape (see Fig. S1B in the supplemental material).

AmpC1 and PenA expression is induced by imipenem. Previously, *bla* gene expression in *B. multivorans* ATCC 17616 was shown to be inducible by β-lactams (13). However, an *E. coli* background was used, only bla_{PenA} induction was evaluated, and induction was measured via nitrocefinase activity. Here, the induction of bla_{AmpC1} and bla_{PenA} expression was assessed via immunoblotting using *B. multivorans* ATCC 17616 grown in lysogeny broth (LB) in the presence of a β-lactam inducer (i.e., 1 μg/ml

TABLE 4 Steady-state kinetic parameters for PenA and AmpC1 with selected β-lactams[a] and avibactam[b]

Compound	β-Lactamase	K_m or $K_{i\ app}$ (μM)	k_{cat} (s^{-1})	k_{cat}/K_m ($\mu M^{-1}\ s^{-1}$)
Cephalothin	PenA[c]	71 ± 7	221 ± 21	3.1 ± 0.3
	AmpC1	392 ± 88	43 ± 5	0.11 ± 0.02
Nitrocefin	PenA[c]	142 ± 14	460 ± 46	3.2 ± 0.3
	AmpC1	176 ± 36	251 ± 25	1.4 ± 0.3
Avibactam	PenA[d]	0.5 ± 0.1	NA[e]	NA
	AmpC1	>600	NA	NA

[a]K_m and k_{cat} were determined under pseudo-1st-order conditions, and a nonlinear least-square fit of the data to the Henri-Michaelis-Menten equation determined the kinetic parameters. Each experiment was completed in triplicate, and the error values represent the standard errors of the mean.
[b]$K_{i\ app}$ was determined using a direct-competition assay under steady-state conditions. Each experiment was completed in triplicate, and the error values represent the standard errors of the mean.
[c]Data were previously published (17).
[d]Data were previously published (20).
[e]NA, not applicable.

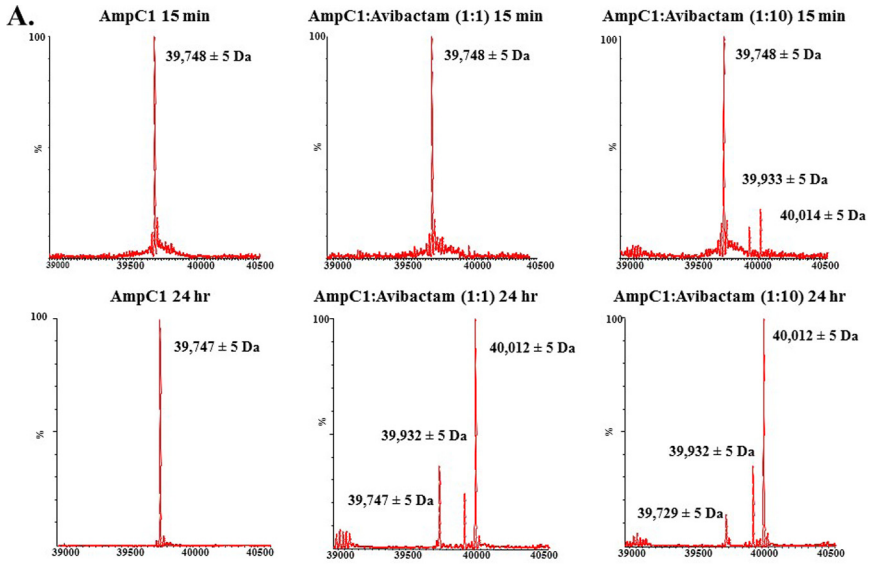

B.

	Sample	Apo – H_2O	Apo	Acyl + 185 Da	Acyl + 265 Da
15 min	AmpC1		39748		
	AmpC1:avibactam (1:1)		39748		
	AmpC1:avibactam (1:10)		39748	39933	40014
24 hr	AmpC1		39747		
	AmpC1:avibactam (1:1)		39747	39932	40012
	AmpC1:avibactam (1:10)	39729		39932	40012

FIG 3 (A) Mass spectrometry of AmpC1 apoenzyme after 15 min (shaded) and 24 h (nonshaded) of incubation. Shown is mass spectrometry of the AmpC1-avibactam acyl-enzyme complex after 15 min and 24 h of incubation at 1:1 and 1:10 enzyme/avibactam ratios. (B) Summary of mass spectrometry data, including description of peaks formed.

imipenem) for different amounts of time (5, 10, 15, 30, 45, 60 75, 90, 105, and 120 min). In the absence of imipenem, PenA protein could not be detected, while a very minor amount of AmpC1 was observed at 75, 90, and 105 min (Fig. 5). The addition of imipenem to the medium resulted in robust expression of AmpC1 and PenA that was time dependent (Fig. 5). The amount of AmpC1 protein produced was greatest between 30 and 90 min and began to decrease by 120 min (Fig. 5). With PenA, at 30 min, the PenA protein level was high, and it remained high up to 120 min (Fig. 5). The presence of 1 μg/ml imipenem in the medium did not alter the growth of *B. multivorans* during the course of the experiment. Expression of bla_{AmpC1} and bla_{PenA} is induced by imipenem, supporting a role for these proteins in β-lactam resistance and/or cell wall recycling and metabolism.

Conclusions. In this study, AmpC1 was found to be a weak β-lactamase. Knocking out bla_{AmpC1} did not impact the susceptibility of *B. multivorans*; however, bla_{AmpC1} expression was induced by imipenem. So, what is the true role of AmpC in *B. multivorans*? Additional investigations are under way to further assess the contribution of AmpC in *B. multivorans*. The catalytic efficiency of one of the 27 variants of AmpC identified here against β-lactams may be greater than that of AmpC1, thus providing a larger contribution to resistance. Alternatively, AmpC may play some role in peptidoglycan metabolism. For example, AmpH class C low-molecular-weight penicillin-binding proteins (PBPs) characterized in *E. coli* possess a structure similar to that of AmpC and have bifunctional DD-carboxypeptidase and DD-endopeptidase activities (23,

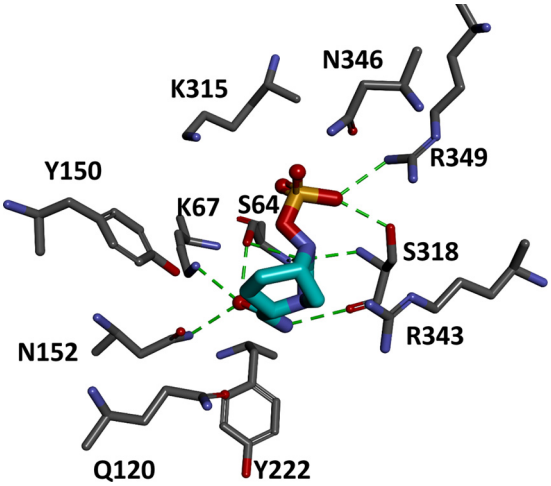

FIG 4 Michaelis-Menten complex of AmpC1 (gray) and avibactam (cyan) revealing nonproductive interactions of avibactam with active-site residues. Potential hydrogen bonding interactions are indicated by dashed green lines.

24). In summary, AmpC from *B. multivorans* is a unique inducible class C cephalosporinase that may play a subsidiary role compared to PenA, which is the dominant β-lactamase.

MATERIALS AND METHODS

Protein analysis. AmpC sequences were analyzed by BLASTP and Bl2Seq from the National Center for Biotechnology Information website. Multiple-sequence alignments were generated using CLUSTAL Ω from the European Bioinformatics Institute (EMBL-EBI) and Discovery Studio (25–27).

Whole-genome sequencing (WGS) of *B. multivorans*. Genomic DNA was purified from the clinical *B. multivorans* isolates using a MasterPure Gram-positive DNA purification kit (Epicentre Inc., Madison, WI) as recommended by the manufacturer. The genomes of 49 *B. multivorans* isolates were sequenced at the J. Craig Venter Institute, Rockville, MD (JCVI) with Illumina NextSeq (two 150-bp reads of sequence data). Paired-end libraries were constructed using Illumina Nextera XT kits. Sequence reads were generated with a target average read depth of ~100-fold coverage. Sequence reads for each isolate were assembled individually using SPAdes (28) and annotated using the National Center for Biotechnology Information (NCBI) Prokaryotic Genome Annotation Pipeline (PGAP) (29). Raw DNA sequence reads were submitted to the NCBI Sequence Read Archive (SRA). A bla_{AmpC} gene could not be found in the AU21596, AU18096, and AU10086 genomes.

Bacterial strains and plasmids. The bla_{AmpC1} gene was synthesized (Celtek Bioscience, LLC) using the deposited nucleotide sequence from *B. multivorans* ATCC 17616 and cloned into pET24a(+) using NdeI and XhoI restriction enzymes. The bla_{AmpC1} gene was subcloned from pET24a(+) to include the ribosomal binding site (RBS) of pET24a(+), using XbaI and XhoI restriction sites; ligated into pBC SK(+); and electroporated in *E. coli* DH10B for susceptibility testing. The bla_{AmpC1} gene was also cloned into pGEX-6P-2 (minus nucleotides 1 to 75, encoding the signal peptide) using BamHI and EcoRI restriction sites and transformed into *E. coli* Rosetta-gami 2 DE3 cells for protein expression. The *B. multivorans* clinical isolates used in this study were obtained from the *Burkholderia cepacia* Research Laboratory and Repository (BcRLR) strain collection (20).

The construction of Δbla_{AmpC1} was conducted using previously described methods (30). Briefly, nucleotide sequences flanking bla_{AmpC1} (630 bp upstream and 432 bp downstream) were synthesized as one fragment by Celtek Bioscience, LLC. An NdeI restriction site was added to the pGPI-SceI vector using

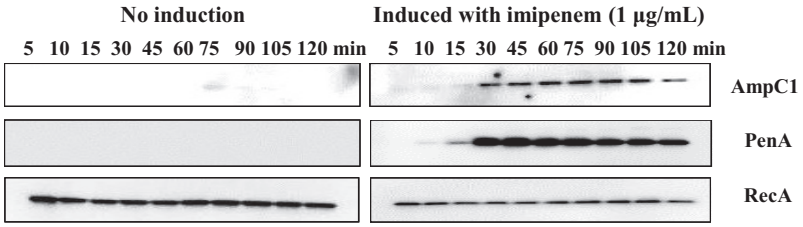

FIG 5 Immunoblotting reveals that protein expression of AmpC1 and PenA is inducible in *B. multivorans* ATCC 17616 after growth in subinhibitory concentrations of imipenem for different amounts of time. The anti-RecA antibody was used as a loading control.

a Quikchange XL kit via site-directed mutagenesis. The bla_{AmpC1} flanking sequence was cloned into the pGPI-SceI vector using XbaI and NdeI restriction sites and transformed into *E. coli* PIR1 cells (Invitrogen). *E. coli* PIR1 containing pGPI-SceI with the flanking sequences was used as the donor strain, and *B. multivorans* ATCC 17616 was used as the recipient strain. The "helper strain" was *E. coli* DH5α(pRK2013). Triparental mating was conducted according to previously published methods (30), and the mixed culture was plated in a single spot on a superoptimal broth (SOB) agar plate containing a nitrocellulose filter and incubated accordingly. The following day, the filter was washed in 1× sterile phosphate-buffered saline (PBS) in order to extract the entire spot of culture and plated onto LB agar with polymyxin B and trimethoprim. The resistant colonies were patched onto phenol red glucose agar plates (5 g peptone, 2.5 g NaCl, 1.8 ml 0.5% phenol red, 7.5 g agar, 50 ml 50% glucose, 450 ml H_2O), and those that did not ferment glucose were subjected to PCR to further confirm the first crossover event. The second crossover was performed as described above, with a different donor strain, *E. coli* DH5α(pDAI-SceI-SacB), using the first-crossover *B. multivorans* as the recipient and *E. coli* DH5α(pRK2013) as the helper. Agar plates containing sucrose were used to cure the pDAI-SceI-SacB plasmid as previously described (30). The resulting knockout strain was confirmed by PCR using primers that lie upstream and downstream of bla_{AmpC}; thus, the final PCR product of the bla_{AmpC} knockout was smaller than the wild type. In addition, internal bla_{AmpC} primers were also used to verify the lack of a PCR product with the knockout and the presence of a PCR product with the wild type. All the PCR products were sequenced for verification.

Analytical isoelectric focusing. *B. multivorans* ATCC 17616 and the Δbla_{AmpC1} strain were grown in LB to an optical density at 600 nm (OD_{600}) of 0.6. A final concentration of 1 μg/ml of imipenem was added to each culture to induce the expression of β-lactamases, and the cultures were grown for 1 h. Cells were pelleted by centrifugation at 12,000 rpm for 10 min. Crude extracts were prepared and loaded onto a FocusGel 3-10 24S (Serva Electrophoresis GmbH) with a pH gradient from 3 to 10 and electrophoresed using a Multiphor II apparatus. The gels were focused at 4°C at 8 W for 120 min. The detection of β-lactamases was performed using an overlay of 2 mM nitrocefin, a chromogenic β-lactam substrate that turns from orange to red upon hydrolysis by a β-lactamase. Purified PenA or AmpC1 β-lactamases were used as controls.

Fluorescence microscopy. *B. multivorans* ATCC 17616 and Δbla_{AmpC1} were grown to an OD_{600} of 0.6 in LB. The cells were pelleted and washed twice in 0.9% NaCl to remove the medium. The cells were resuspended to an OD_{600} of 1.25 in 1 ml of 0.9% NaCl and stained for 15 min in the dark using LIVE/DEAD BacLight bacterial viability kits (Molecular Probes; L7012) with equal ratios of SYTO9 (3 μl) and propidium iodide (3 μl) stains, according to the manufacturer's instructions. Three microliters of each sample was placed onto a glass slide with a coverslip. Samples were viewed on a Zeiss Axio Imager M1 microscope with a metal halide arc lamp using the green fluorescent protein (GFP) and DSRED filters, and images were obtained at ×400 and ×1,000 (oil immersion) magnification.

Antibiotic susceptibility. Mueller-Hinton (M-H) agar dilution MICs, according to the Clinical and Laboratory Standards Institute (CLSI) (31, 32), were used to phenotypically characterize strains, as previously described (32).

Protein expression and purification of AmpC1. *E. coli* Rosetta 2 DE3 or Origami 2 DE3 cells producing the AmpC1 β-lactamase from the pGEX-6P-2 plasmid were grown, lysed, and processed as previously described (33, 34). The recombinant AmpC1 possesses a cleavable N-terminal glutathione *S*-transferase (GST) tag, and thus, the crude extracts were run on a GSTrap FF column (GE LifeSciences). The GST tag was cleaved using PreScission protease as previously described (33, 34). The purity of the fractions was determined by sodium dodecyl sulfate-polyacrylamide gel electrophoresis (SDS-PAGE). Gels were stained with Coomassie brilliant blue R250, and the protein's mass was verified via ESI-MS. Protein concentrations were determined by measuring absorbance at a wavelength of 280 nm (λ_{280}) and using the protein's extinction coefficient ($\Delta\varepsilon$) (49,850 M^{-1} cm^{-1} at 280 nm), which was obtained using the ProtParam tool available through the ExPASy Bioinformatics Resource Portal (31). To maintain full activity, AmpC1 was stored in 10 mM PBS, pH 7.4, with 25% glycerol at −20°C. Three milligrams of purified AmpC1 was sent to New England Peptide for antibody production in rabbits.

Kinetics. Steady-state kinetic parameters were determined using an Agilent 8453 diode array spectrophotometer, as previously described (32, 35). Enzfitter (Biosoft) was used to fit the data to the Henri-Michaelis-Menten equation and to obtain the kinetic parameters, V_{max} and K_m, for the β-lactam substrates, nitrocefin and cephalothin, as follows: $v = (V_{max} \times [S])/(K_m + [S])$, where v indicates velocity and [S] indicates concentration of substrate.

Using a direct-competition assay under steady-state conditions, the $K_{i\ app}$ of avibactam was determined for AmpC1 as previously described (32, 35). The data were analyzed according to the following equation to account for the affinity of nitrocefin ([S], ncf) for the lactamase: $K_{i\ app}$ (corrected) = $K_{i\ app}$ (observed)/(1 + [S]/K_m ncf).

ESI-MS. ESI-MS was conducted on a Waters Synapt G2-Si as previously described (20). Purified AmpC1 was incubated with either a 1:1 or 1:10 enzyme/inhibitor ratio with avibactam. Reactions were terminated by the addition of 0.1% formic acid and acetonitrile.

Molecular modeling. The AmpC1 homology model was generated using the SWISS-MODEL repository with the *B. cenocepacia* AmpC crystal structure (PDB accession no. 5E2G) as the template (identity, 298/389 [77%]; similarity, 320/389 [82%]) (36–38). The local quality of the AmpC1 model was estimated using the raw QMEAN scoring function and was found to be 0.7 (39–41). The majority of the residues in AmpC1 had a QMEAN score of 0.8 (1 is maximum for the best model). However, the score for the L117-to-H126 loop was 0.3, indicating that the positioning of the loop was not reliable. The L117-to-H126 loop sits at the entrance to the AmpC1 active site; thus, the model required further refinement. A

second homology model generated via the SWISS-MODEL repository had an overall QMEAN score for the protein of 0.73, and the scores for the residues in the L117-to-H126 loop were between 0.6 and 0.8. Around amino acid 300, the QMEAN score was near 0.3; however, the overall quality of the second model, especially for the residues near the active site, was much better. A multistep CHARMm protocol using an *ab initio* loop prediction algorithm, LOOPER, in BIOVIA Discovery Studio 2017 (DS2017) R2 (Accelrys, Inc. San Diego, CA) was used to generate a set of low-energy conformations for the specified loop region (L117 to H126), and they were scored based on their CHARMm energy. The best-scoring conformation was very similar to that of the second model. Thus, the second AmpC1 model used to construct Michaelis-Menten complexes with avibactam as previously described, using BIOVIA DS2017 molecular-modeling software (32). Intact and acylated avibactams were constructed using Fragment Builder tools and minimized using a Standard Dynamics Cascade protocol of DS2017. The avibactam was automatically docked into the active site of AmpC1 using the CDOCKER module of DS2017 (42).

Cloning, protein expression, and purification of *recA*. The *recA* gene was amplified from genomic DNA isolated from *B. multivorans* ATCC 17616. The PCR product obtained was cloned into the pCR-XL-TOPO vector (Invitrogen) and electroporated into *E. coli* TOP10. The pGEX-6P-2 empty vector (allowing for the addition of a cleavable N-terminal GST tag) and pCR-XL-TOPO *recA* were digested using BamHI and XhoI restriction enzymes. The digested products, corresponding to pGEX-6P-2 and *recA*, were ligated overnight at 22°C, and the ligation reaction product was electroporated into *E. coli* DH10B. The pGEX-6P-2 *recA* plasmid was verified by DNA sequencing using MCLab. For protein expression, the pGEX-6P-2 *recA* plasmid was transformed into *E. coli* Rosetta 2 DE3 cells (Novagen). The RecA protein purification was conducted as described above for AmpC. The protein concentrations were determined by measuring the absorbance at λ_{280} and using the protein's extinction coefficient ($\Delta\varepsilon$, 14,440 M^{-1} cm^{-1} for RecA at λ_{280}). The theoretical mass of RecA (37,765 Da), as well as the extinction coefficient, was obtained using the ProtParam tool on the ExPASy Bioinformatics Resource Portal (31). Three milligrams of purified RecA was sent to New England Peptide for antibody production in rabbits.

Immunoblotting and induction of β-lactamase expression. To measure β-lactamase induction, immunoblotting was conducted using the polyclonal AmpC1, PenA peptide (18), and RecA antibodies. *B. multivorans* ATCC 17616 was grown in LB to log phase at an OD_{600} between 0.6 and 0.7. *B. multivorans* ATCC 17616 was treated with 1 μg/ml of imipenem to induce expression of bla_{penA} and bla_{AmpC1}, and aliquots of cells were collected after 5, 10, 15, 30, 45, 60, 75, 90, 105, and 120 min of induction. *B. multivorans* cells not induced with imipenem at the above-mentioned time points were also collected. Subsequently, the cells were pelleted and lysed using stringent periplasmic fractionation to prepare lysates, as previously described (43). These crude extracts were subjected to SDS-PAGE and transferred to polyvinylidene difluoride membranes. The membranes were blocked in 5% nonfat dry milk in 20 mM Tris-Cl with 150 mM NaCl, pH 7.4 (TBS), for 1 h and probed in 5% nonfat dry milk in TBS with 1 μg/ml of polyclonal AmpC, PenA peptide, or RecA antibodies. The membranes were washed five times for 10 min each time with TBS with 0.05% Tween 20 (TBST), and for protein detection, blots were incubated for 1 h in 1:5,000 dilutions of anti-rabbit secondary horseradish peroxidase (HRP)-conjugated antibodies in 5% nonfat dry milk in TBS. The immunoblots were washed five times for 10 min each time with TBST and developed using an ECL-Plus developing kit (GE Healthcare Life Sciences) or SuperSignal West Femto chemiluminescent substrate (Thermo Scientific) according to the manufacturers' instructions. Fotodyne Luminary/FX was used to capture images.

Accession number(s). Annotated genomes were deposited in the GenBank WGS repository and can be obtained within BioProject PRJNA434393.

SUPPLEMENTAL MATERIAL

Supplemental material for this article may be found at https://doi.org/10.1128/AAC.01140-18.

SUPPLEMENTAL FILE 1, PDF file, 1.5 MB.

ACKNOWLEDGMENTS

The pGPI-SceI, pRK2013, and pDAI-SceI-SacB plasmids were kind gifts from Miguel Valvano of Queen's University Belfast. We thank Brett Hanzlicek for assistance with fluorescence microscopy.

Research reported in this article was supported in part by funds and/or facilities provided by the Cleveland Department of Veterans Affairs, the Veterans Affairs Merit Review Program (BX002872 to K.M.P.-W. from the U.S. Department of Veterans Affairs Biomedical Laboratory Research and Development Service). This project has been funded in whole or in part with federal funds from the National Institute of Allergy and Infectious Diseases, National Institutes of Health, Department of Health and Human Services under awards U19AI110819 to the JCVI and U19AI109713-SRP to K.M.P.-W. This work was also supported by funding (to J.J.L.) from the Cystic Fibrosis Foundation.

The contents do not represent the views of the U.S. Department of Veterans Affairs or the United States government. The content is solely our responsibility and does not necessarily represent the official views of the National Institutes of Health.

REFERENCES

1. Mahenthiralingam E, Vandamme P. 2005. Taxonomy and pathogenesis of the *Burkholderia cepacia* complex. Chron Respir Dis 2:209–217. https://doi.org/10.1191/1479972305cd053ra.
2. Vandamme P, Dawyndt P. 2011. Classification and identification of the *Burkholderia cepacia* complex: past, present and future. Syst Appl Microbiol 34:87–95. https://doi.org/10.1016/j.syapm.2010.10.002.
3. Marson FA, Hortencio TD, Aguiar KC, Ribeiro JD. 2015. Demographic, clinical, and laboratory parameters of cystic fibrosis during the last two decades: a comparative analysis. BMC Pulm Med 15:3. https://doi.org/10.1186/1471-2466-15-3.
4. Abbott IJ, Peleg AY. 2015. *Stenotrophomonas*, *Achromobacter*, and nonmelioid *Burkholderia* species: antimicrobial resistance and therapeutic strategies. Semin Respir Crit Care Med 36:99–110. https://doi.org/10.1055/s-0034-1396929.
5. Hanulik V, Webber MA, Chroma M, Uvizl R, Holy O, Whitehead RN, Baugh S, Matouskova I, Kolar M. 2013. An outbreak of *Burkholderia multivorans* beyond cystic fibrosis patients. J Hosp Infect 84:248–251. https://doi.org/10.1016/j.jhin.2013.04.001.
6. Chiappini E, Taccetti G, de Martino M. 2014. Bacterial lung infections in cystic fibrosis patients: an update. Pediatr Infect Dis J 33:653–654. https://doi.org/10.1097/INF.0000000000000347.
7. Gautam V, Singhal L, Ray P. 2011. *Burkholderia cepacia* complex: beyond *Pseudomonas* and *Acinetobacter*. Indian J Med Microbiol 29:4–12. https://doi.org/10.4103/0255-0857.76516.
8. Avgeri SG, Matthaiou DK, Dimopoulos G, Grammatikos AP, Falagas ME. 2009. Therapeutic options for *Burkholderia cepacia* infections beyond cotrimoxazole: a systematic review of the clinical evidence. Int J Antimicrob Agents 33:394–404. https://doi.org/10.1016/j.ijantimicag.2008.09.010.
9. Wuthiekanun V, Peacock SJ. 2006. Management of melioidosis. Expert Rev Anti Infect Ther 4:445–455. https://doi.org/10.1586/14787210.4.3.445.
10. Cheung TK, Ho PL, Woo PC, Yuen KY, Chau PY. 2002. Cloning and expression of class A β-lactamase gene *blaA*(BPS) in *Burkholderia pseudomallei*. Antimicrob Agents Chemother 46:1132–1135. https://doi.org/10.1128/AAC.46.4.1132-1135.2002.
11. Godfrey AJ, Wong S, Dance DA, Chaowagul W, Bryan LE. 1991. *Pseudomonas pseudomallei* resistance to β-lactam antibiotics due to alterations in the chromosomally encoded β-lactamase. Antimicrob Agents Chemother 35:1635–1640. https://doi.org/10.1128/AAC.35.8.1635.
12. Tribuddharat C, Moore RA, Baker P, Woods DE. 2003. *Burkholderia pseudomallei* class A β-lactamase mutations that confer selective resistance against ceftazidime or clavulanic acid inhibition. Antimicrob Agents Chemother 47:2082–2087. https://doi.org/10.1128/AAC.47.7.2082-2087.2003.
13. Trepanier S, Prince A, Huletsky A. 1997. Characterization of the *penA* and *penR* genes of *Burkholderia cepacia* 249 which encode the chromosomal class A penicillinase and its LysR-type transcriptional regulator. Antimicrob Agents Chemother 41:2399–2405.
14. Bush K, Jacoby GA. 2010. Updated functional classification of β-lactamases. Antimicrob Agents Chemother 54:969–976. https://doi.org/10.1128/AAC.01009-09.
15. Poirel L, Rodriguez-Martinez JM, Plesiat P, Nordmann P. 2009. Naturally occurring class A β-lactamases from the *Burkholderia cepacia* complex. Antimicrob Agents Chemother 53:876–882. https://doi.org/10.1128/AAC.00946-08.
16. Dhar S, Kumari H, Balasubramanian D, Mathee K. 2018. Cell-wall recycling and synthesis in *Escherichia coli* and *Pseudomonas aeruginosa*—their role in the development of resistance. J Med Microbiol 67:1–21. https://doi.org/10.1099/jmm.0.000636.
17. Papp-Wallace KM, Taracila MA, Gatta JA, Ohuchi N, Bonomo RA, Nukaga M. 2013. Insights into β-lactamases from *Burkholderia* species, two phylogenetically related yet distinct resistance determinants. J Biol Chem 288:19090–19102. https://doi.org/10.1074/jbc.M113.458315.
18. Becka SA, Zeiser ET, Marshall SH, Gatta JA, Nguyen K, Singh I, Sutton G, Greco C, Fouts DE, LiPuma JJ, Papp-Wallace KM. 18 June 2018. Sequence heterogeneity of the PenA carbapenemase in clinical isolates of *Burkholderia multivorans*. Diagn Microbiol Infect Dis. https://doi.org/10.1016/j.diagmicrobio.2018.06.005.
19. Jacoby GA. 2009. AmpC β-lactamases. Clin Microbiol Rev 22:161–182. https://doi.org/10.1128/CMR.00036-08.
20. Papp-Wallace KM, Becka SA, Zeiser ET, Ohuchi N, Mojica MF, Gatta JA, Falleni M, Tosi D, Borghi E, Winkler ML, Wilson BM, LiPuma JJ, Nukaga M, Bonomo RA. 2017. Overcoming an extremely drug resistant (XDR) pathogen: avibactam restores susceptibility to ceftazidime for *Burkholderia cepacia* complex isolates from cystic fibrosis patients. ACS Infect Dis 3:502–511. https://doi.org/10.1021/acsinfecdis.7b00020.
21. Bulychev A, Mobashery S. 1999. Class C β-lactamases operate at the diffusion limit for turnover of their preferred cephalosporin substrates. Antimicrob Agents Chemother 43:1743–1746.
22. Ehmann DE, Jahic H, Ross PL, Gu RF, Hu J, Durand-Reville TF, Lahiri S, Thresher J, Livchak S, Gao N, Palmer T, Walkup GK, Fisher SL. 2013. Kinetics of avibactam inhibition against class A, C, and D β-lactamases. J Biol Chem 288:27960–27971. https://doi.org/10.1074/jbc.M113.485979.
23. Sauvage E, Kerff F, Terrak M, Ayala JA, Charlier P. 2008. The penicillin-binding proteins: structure and role in peptidoglycan biosynthesis. FEMS Microbiol Rev 32:234–258. https://doi.org/10.1111/j.1574-6976.2008.00105.x.
24. Gonzalez-Leiza SM, de Pedro MA, Ayala JA. 2011. AmpH, a bifunctional DD-endopeptidase and DD-carboxypeptidase of *Escherichia coli*. J Bacteriol 193:6887–6894. https://doi.org/10.1128/JB.05764-11.
25. Sievers F, Wilm A, Dineen D, Gibson TJ, Karplus K, Li W, Lopez R, McWilliam H, Remmert M, Soding J, Thompson JD, Higgins DG. 2011. Fast, scalable generation of high-quality protein multiple sequence alignments using Clustal Ω. Mol Syst Biol 7:539. https://doi.org/10.1038/msb.2011.75.
26. Li W, Cowley A, Uludag M, Gur T, McWilliam H, Squizzato S, Park YM, Buso N, Lopez R. 2015. The EMBL-EBI bioinformatics web and programmatic tools framework. Nucleic Acids Res 43:W580–W584. https://doi.org/10.1093/nar/gkv279.
27. McWilliam H, Li W, Uludag M, Squizzato S, Park YM, Buso N, Cowley AP, Lopez R. 2013. Analysis tool web services from the EMBL-EBI. Nucleic Acids Res 41:W597–W600. https://doi.org/10.1093/nar/gkt376.
28. Bankevich A, Nurk S, Antipov D, Gurevich AA, Dvorkin M, Kulikov AS, Lesin VM, Nikolenko SI, Pham S, Prjibelski AD, Pyshkin AV, Sirotkin AV, Vyahhi N, Tesler G, Alekseyev MA, Pevzner PA. 2012. SPAdes: a new genome assembly algorithm and its applications to single-cell sequencing. J Comput Biol 19:455–477. https://doi.org/10.1089/cmb.2012.0021.
29. Tatusova T, DiCuccio M, Badretdin A, Chetvernin V, Nawrocki EP, Zaslavsky L, Lomsadze A, Pruitt KD, Borodovsky M, Ostell J. 2016. NCBI prokaryotic genome annotation pipeline. Nucleic Acids Res 44:6614–6624. https://doi.org/10.1093/nar/gkw569.
30. Aubert DF, Hamad MA, Valvano MA. 2014. A markerless deletion method for genetic manipulation of *Burkholderia cenocepacia* and other multidrug-resistant Gram-negative bacteria. Methods Mol Biol 1197:311–327. https://doi.org/10.1007/978-1-4939-1261-2_18.
31. Gasteiger E, Hoogland C, Gattiker A, Duvaud S, Wilkins MR, Appel RD, Bairoch A. 2005. The proteomics protocols handbook. Humana Press, New York, NY.
32. Papp-Wallace KM, Bethel CR, Distler AM, Kasuboski C, Taracila M, Bonomo RA. 2010. Inhibitor resistance in the KPC-2 β-lactamase, a preeminent property of this class A β-lactamase. Antimicrob Agents Chemother 54:890–897. https://doi.org/10.1128/AAC.00693-09.
33. Papp-Wallace KM, Becka SA, Taracila MA, Zeiser ET, Gatta JA, LiPuma JJ, Bonomo RA. 2017. Exploring the role of the Ω-loop in the evolution of ceftazidime resistance in the PenA β-lactamase from *Burkholderia multivorans*, an important cystic fibrosis pathogen. Antimicrob Agents Chemother 61:e01941-16. https://doi.org/10.1128/AAC.01941-16.
34. Winkler ML, Rodkey EA, Taracila MA, Drawz SM, Bethel CR, Papp-Wallace KM, Smith KM, Xu Y, Dwulit-Smith JR, Romagnoli C, Caselli E, Prati F, van den Akker F, Bonomo RA. 2013. Design and exploration of novel boronic acid inhibitors reveals important interactions with a clavulanic acid-resistant sulfhydryl-variable (SHV) β-lactamase. J Med Chem 56:1084–1097. https://doi.org/10.1021/jm301490d.
35. Papp-Wallace KM, Taracila M, Wallace CJ, Hujer KM, Bethel CR, Hornick JM, Bonomo RA. 2010. Elucidating the role of Trp105 in the KPC-2 β-lactamase. Protein Sci 19:1714–1727. https://doi.org/10.1002/pro.454.
36. Bienert S, Waterhouse A, de Beer TA, Tauriello G, Studer G, Bordoli L, Schwede T. 2017. The SWISS-MODEL repository; new features and functionality. Nucleic Acids Res 45:D313–D319. https://doi.org/10.1093/nar/gkw1132.
37. Biasini M, Bienert S, Waterhouse A, Arnold K, Studer G, Schmidt T, Kiefer F, Gallo Cassarino T, Bertoni M, Bordoli L, Schwede T. 2014. SWISS-

MODEL: modelling protein tertiary and quaternary structure using evolutionary information. Nucleic Acids Res 42:W252–W258. https://doi.org/10.1093/nar/gku340.
38. Guex N, Peitsch MC, Schwede T. 2009. Automated comparative protein structure modeling with SWISS-MODEL and Swiss-PDBViewer: a historical perspective. Electrophoresis 30(Suppl 1):S162–S173. https://doi.org/10.1002/elps.200900140.
39. Benkert P, Tosatto SC, Schomburg D. 2008. QMEAN: a comprehensive scoring function for model quality assessment. Proteins 71:261–277. https://doi.org/10.1002/prot.21715.
40. Benkert P, Biasini M, Schwede T. 2011. Toward the estimation of the absolute quality of individual protein structure models. Bioinformatics 27:343–350. https://doi.org/10.1093/bioinformatics/btq662.
41. Bertoni M, Kiefer F, Biasini M, Bordoli L, Schwede T. 2017. Modeling protein quaternary structure of homo- and hetero-oligomers beyond binary interactions by homology. Sci Rep 7:10480. https://doi.org/10.1038/s41598-017-09654-8.
42. Wu G, Robertson DH, Brooks CL, Vieth M. 2003. Detailed analysis of grid-based molecular docking: a case study of CDOCKER—a CHARMm-based MD docking algorithm. J Comput Chem 24:1549–1562. https://doi.org/10.1002/jcc.10306.
43. Papp-Wallace KM, Taracila MA, Smith KM, Xu Y, Bonomo RA. 2012. Understanding the molecular determinants of substrate and inhibitor specificities in the carbapenemase KPC-2: exploring the roles of Arg220 and Glu276. Antimicrob Agents Chemother 56:4428–4438. https://doi.org/10.1128/AAC.05769-11.